Integrated Bidding and Operating Strategies for Wind-Storage Systems

Huajie Ding, *Student Member, IEEE*, Pierre Pinson, *Senior Member, IEEE*, Zechun Hu, *Member, IEEE* and Yonghua Song, *Fellow, IEEE*

***Abstract*—Due to their flexible charging and discharging capabilities, energy storage systems (ESS) are considered a promising complement to wind farms participating in electricity markets. This paper presents integrated day-ahead bidding and real-time operation strategies for a wind-storage system to perform arbitrage and to alleviate wind power deviations from day-ahead contracts. The strategy is developed with two-price balancing markets in mind. A mixed integer nonlinear optimization formulation is built to determine optimal offers by taking into account expected wind power forecasting errors and the power balancing capability of the ESS. A modified gradient descent algorithm is designed to solve this nonlinear problem. A number of case studies validate the computational efficiency and optimality of the algorithm. Compared to the existing strategies, the proposed strategies yield increased economic profit, regardless of the temporal dependence of wind power forecasting errors.**

***Index Terms*—Bidding strategy, electricity markets, energy storage system, real-time operation, wind farm**

I. Nomenclature

Index sets:

$t=\{1,2\ldots T\}$	Set of time intervals.
$k=\{1,2\ldots K\}$	Set of iterations for the algorithm.

Functions:

$S_t(\cdot)$	Probabilistic profit for interval *t*.
$w_t(\cdot)$	Probabilistic density function of wind power forecast for interval *t*.
$W_t(\cdot)$	Cumulative distribution function of wind power forecast for interval *t*.
$W_t^{-1}(\cdot)$	Inverse function of $W_t(\cdot)$.

Variables:

B_t^D	Day-ahead bidding for interval *t*.
BS_t^C, BS_t^D	Charging and discharging reserve capacity of energy storage for interval *t*.
p_t	Wind power generation for interval *t*.
p_t^{ch}, p_t^{dis}	Charging and discharging power of energy storage for interval *t*.
$u_t^C,\ u_t^D$	Binary variables indicating charging and discharging status of storage for interval *t*.
E_t	Residual energy of storage for interval *t*.
γ	Step size of gradient descending algorithm.
β	Back-tracking factor in the algorithm

Constants:

Δt	Duration of a time interval
$\overline{wf_t},\ \underline{wf_t}$	Upper and lower bounds of wind power forecast for interval *t*.
$\overline{\lambda}_t^D$	Expected day-ahead price for interval *t*.
$\overline{\lambda}_t^{up}, \overline{\lambda}_t^{dw}$	Expected up/down-regulation prices for interval *t*.
T	Maximal number of market time units.
η_c, η_d	Energy efficiency of charging and discharging process.
$E_{\min}, E_{\max}$	Minimal and maximal level of residual energy of energy storage.
$\overline{BS^C}, \overline{BS^D}$	Upper bounds of charging and discharging reserve of ESS.
C_{WF-ESS}	Integration capacity of wind-storage system
C_{WF}, C_{ESS}	Integration capacity of wind farm and energy storage

II. Introduction

Recent decades have witnessed the rapid development of wind power generation. To better accommodate wind energy in existing power systems, a consensus has been gradually reached such that the increasing capacity of wind power should be traded in day-ahead markets [1] [2]. Because of the limited predictability of wind power, optimal offering strategies for wind farms (WF) in day-ahead electricity markets have been widely studied. As a first representative example, Reference [1] proposes a closed-form optimal day-ahead bidding strategy, considering stochastics in both prices and wind generation, which has advantages over LP-type models in terms of the transparency of results, computational efficiency and reduced data requirement. Moreover, Reference [3] extends the *expected utility maximization (EUM) strategy* with a more general loss function to express the economic loss of the WF resulting from potential deviations from day-ahead contracts. This loss function is also relevant in the cases where WFs coordinate with conventional generators, even though it overlooks temporal dependencies. The authors of [4] anchor the bidding amounts within a certain neighborhood of deterministic forecast values to account for risk aversion while improving the EUM strategy. This can alleviate risky bidding in electricity markets, which may result in large imbalances and endanger power system stability.

The limited accuracy of wind power forecasts results in revenue loss for wind power producers because they should buy up-regulation (additional energy sold by other

This research work was supported in part by the National Natural Science Foundation of China (51107060) and the Chinese Scholarship Council. Pierre Pinson is partly supported by the Danish Strategic Council for Strategic Research through the projects of PROAIN (no. 3045-00012B/DSF) and 5s - Future Electricity Markets (no. 12-132636/DSF).

Huajie Ding, Zechun Hu and Yonghua Song are with the state key Lab of Power Systems, Department of Electrical Engineering, Tsinghua University, Beijing, 100084, China (e-mail: dinghj13@mails.tsinghua.edu.cn, zechhu@tsinghua.edu.cn, yhsong@tsinghua.edu.cn).

Pierre Pinson is with the Department of Electrical Engineering, Technical University of Denmark, Lyngby, DK-2800, Denmark (e-mail: ppin@dtu.dk).

participants) or sell down-regulation (energy bought by other participants) in balancing markets to settle their deviations between day-ahead offers and actual power output [5], [6]. Energy storage systems (ESS) can hence be regarded as a suitable complement to wind power because they allow flexible charging and discharging to accommodate imbalances. ESS can coordinate with WF in two ways. On one hand, because ESS make arbitrage with variable prices, the overall profit of WF and ESS can increase in day-ahead markets compared with the situation where they are considered separately. The coordination of WF and ESS to make arbitrage in regulated electricity markets has been studied in [7] and [8] (among others), with and without intraday markets considered, respectively. More specifically, the ability of pumped storage plants to reduce the wind spillage and make arbitrage is studied in [9]. However, the formulation does not consider market penalties for imbalances, which is different from current rules in deregulated electricity markets. On the other hand, ESS can help flatten the variations of WF output in real-time operation [10]–[12]. A *filter operation strategy* is stated in [13], which utilizes ESS to compensate for the imbalance from day-ahead offering [14]. Similarly, the so-called *reserve operation strategy* is proposed in [15], which also uses the *EUM* strategy at the offering stage but then sets contracts for ESS to cover the shortfalls of WFs. The work in [16] shows that WFs and ESS can both be better off through contracts for compensation of wind power deviations by ESS. The concavity of objective functions based on the greedy control strategy of ESS is studied. Although the potential arbitrage strategy of ESS is overlooked, it certainly influences day-ahead offerings and resulting market revenues.

The main contributions of this paper consist of proposing integrated day-ahead bidding and real-time operation strategies for wind-storage systems (abbreviated WF-ESS) as a price taker. The cooperative strategy is that ESS sets charging or discharging reserve capacities at each time interval up to which the ESS can compensate for potential imbalances from the wind farm. Although sometimes ESS cannot compensate for imbalance due to the presetting operation mode, fixing the charging/discharging status for each hour can avoid the frequent mode switching of ESS. Furthermore, the cooperative strategy is simple such that it is suitable for integrating it into day-ahead bidding optimization. Based on this cooperative strategy and using a price-taker assumption, a stochastic optimization model is proposed to maximize the expected profit. The method could be extended in the future to relax the price-taker assumption used here. Similarly, degradation costs are not accounted for in the design of offering strategies (as for most of the literature on this topic), even though it could be readily included in the future. An additional contribution relates to the proposal of a computationally efficient algorithm to solve the optimization problem resulting from our formulations. Furthermore, a number of case studies are used to study the influence of the temporal dependence structure of wind power errors on revenues from the market.

This paper is organized as follows. Section III gives a brief introduction regarding day-ahead and balancing markets. Based on existing market rules, day-ahead bidding and real-time operation strategies are formulated. Section IV proposes a modified gradient descent algorithm to solve the optimization problem. In Section V, an illustrative case study with three market time units only and simplified assumptions on wind power forecast uncertainty are first employed to demonstrate the computational efficiency and optimality of the proposed solving method. Subsequently, another case study based on realistic data compares the profit from the application of our proposed strategies with other common ones from the literature. Conclusions and perspectives for future work are gathered in Section VI.

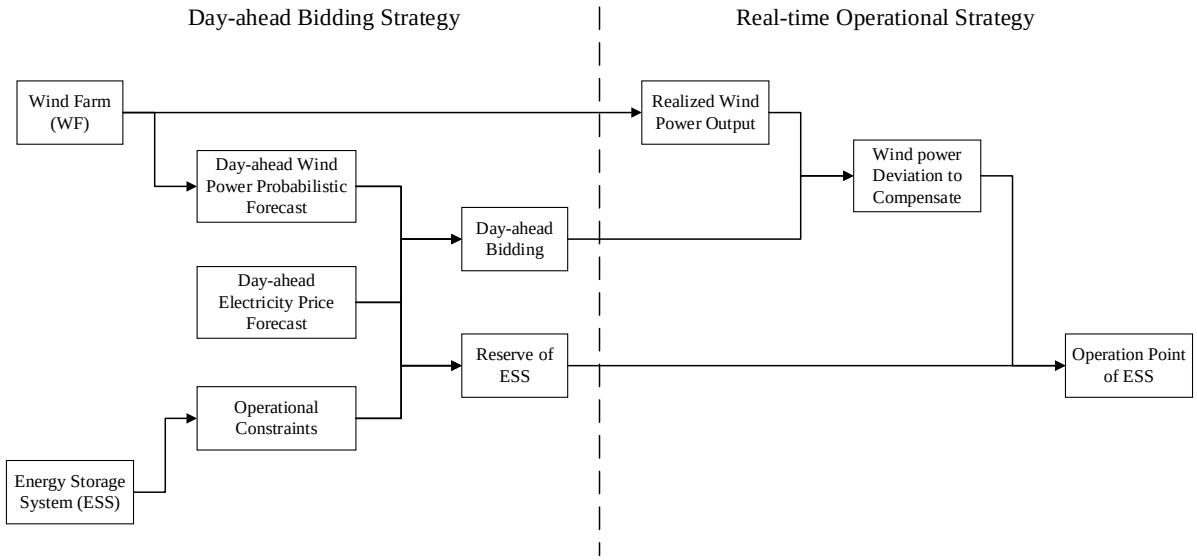

Fig. 1 Schematic illustration of day-ahead bidding strategy and real-time operating strategy of wind farm and energy storage system

III. Optimal Bidding and Control Strategy

A. Imbalance Management in Electricity Markets

In most deregulated electricity energy markets such as the Scandinavian Nord Pool, participants should trade in both day-ahead and balancing markets. Intra-day markets (or adjustment markets) also exist between day-ahead and balancing stages, which provide a platform for transactions on renewable energy generation [17]. However, because the trading amount in these markets is relatively small, it is not

considered in this paper. Recent work on intra-day markets for wind power producers can be found in [18].

In the day-ahead market, power plants bid for their generation schedule that covers the following day with 12 to 14 hours prior to actual operation [19]. The cleared schedules are subject to deviation penalties, which means that the participants need to buy or sell up/down regulation services for any deviation in actual output from schedules in the balancing market. Balancing markets can be divided into two categories according to whether the balancing price changes with the overall imbalance sign [20]. The deviation is traded at a unique price in one-price balancing markets, which is adopted in markets such as the Dutch APX [21]. In the two-price markets such as Nord Pool and the Iberian market, deviation that is opposite to the system imbalance is traded at the day-ahead price while the imbalance of the same sign with that of the system is traded at the cleared balancing price. The model proposed in this paper is based on the second one because it is more comprehensive.

B. Day-ahead Bidding Strategy

The day-ahead bidding strategy of WF-ESS is usually the same as what is utilized by WF when it works alone [10]–[12]. The ESS is only used to compensate for the deviation between day-ahead offers and real-time output. The WF-ESS can then be regarded as a conventional generation plant. In fact, ESS has the ability to make arbitrage in combination with compensating for imbalances. Consequently, the arbitrage and balancing functions of ESS are both considered in our day-ahead optimization model. In the present approach, it is the WF-ESS union that bids in the day-ahead market rather than the WF or ESS alone as in [13]. Therefore, the optimal bidding of the union will no longer be the specific quantile of the wind power probabilistic forecast [3]. As shown in Fig. 1, the inputs of the optimization model for day-ahead bidding include wind power probabilistic forecasts, day-ahead prices (including up and down-regulation prices) forecasts and operational constraints of the ESS. The model then determines the optimal bidding in the market and the reserve from the ESS for the various market time units.

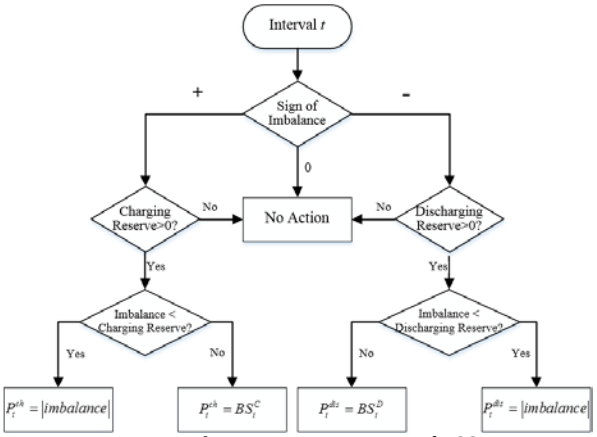

Fig. 2 Real-time operating strategy of ESS

C. Real-time Operating Strategy

Only compensating for the imbalance by ESS in real-time operation may risk charging at high prices but discharging at low prices. Moreover, the imperfect round-trip efficiency of ESS would further reduce the potential profit of the union. It is natural to consider that the situation will be improved if there are some constraints on the charging and discharging power at each time interval.

In this paper, a reserve-based operating strategy is proposed. As shown in Fig. 1, the charging or discharging status of the ESS at each time interval is optimized in advance, which means the ESS works only if the real-time imbalance sign of the WF output goes with the predetermined working status. Furthermore, it also sets constraints on the charging and discharging power, which can be considered as the operational reserve provided for the WF by the ESS. This means that even if the deviation of WF exceeds the reserve capacity, the ESS can charge or discharge at most to the predetermined upper bounds, which are often lower than the ones determined by the operational constraints. By this method, the ESS can avoid charging at high-price intervals or discharging at low-price periods.

The detailed flow chart of the real-time operating strategy of ESS is depicted in Fig. 2. Take the decision procedure of charging for example. When the generated wind power at interval *t* is higher than the bidding value, it is referred to as the *positive imbalance* of WF (symbolized as '+'), while the opposite situation is called the *negative imbalance* (symbolized as '−'). In positive imbalance cases, if the ESS has predetermined the charging reserve from the day-ahead optimization, the charging power of ESS can be set as the minimum of the imbalance and reserve. Otherwise, the ESS takes no action. The decision procedure of the discharging action is similar to that of the charging action.

D. Formulations of Bidding and Operating Strategies

Based on the aforementioned bidding and operating strategies, the optimal bidding and charging/discharging reserve can be generally formulated as

$$\begin{aligned} \max_{\theta} \quad & f(\boldsymbol{\theta}) \\ \text{s.t.} \quad & h(\boldsymbol{\theta}) \le 0 \\ & g(\boldsymbol{\theta}) \le 0 \end{aligned} \tag{1}$$

where $\boldsymbol{\theta} = \left\{ \boldsymbol{B^D}, \boldsymbol{BS^C}, \boldsymbol{BS^D} \right\}$ are decision variables. Sequentially, $\boldsymbol{B^D}, \boldsymbol{BS^C}, \boldsymbol{BS^D}$ are vectors of day-ahead bidding B_t^D, charging reserve BS_t^C and discharging reserve BS_t^D. The objective function $f(\boldsymbol{\theta})$ is the expected profit from the WF-ESS, while $h(\boldsymbol{\theta}) \le 0$ and $g(\boldsymbol{\theta}) \le 0$ are constraints on the bidding and operation of the ESS.

The objective of the ESS operation is to make arbitrage and to compensate for the potential imbalances of the wind farm. Wind power generation p_t at time interval *t* follows a distribution described by its probability density function $w_t(p_t)$. Then, the expected profit $f(\boldsymbol{\theta})$ at all *T* intervals can be written as,

$$f(\boldsymbol{\theta}) = \sum_{t=1}^{T} E\left[S_t(p) \,\middle|\, \lambda_t^D, \lambda_t^{up}, \lambda_t^{dw}, \theta_t \right] \Delta t \tag{2}$$

where

$$E\left[S_t(p)\,\middle|\,\lambda_t^D,\lambda_t^{up},\lambda_t^{dw},\theta_t\right]$$
$$=\overline{\lambda}_t^D B_t^D+\overline{\lambda}_t^{up}\int_{\underline{wf_t}}^{B_t^D-BS_t^D}\left(p-B_t^D+BS_t^D\right)w_t(p)\,dp \qquad (3)$$
$$+\overline{\lambda}_t^{dw}\int_{B_t^D+BS_t^C}^{\overline{wf_t}}\left(p-B_t^D-BS_t^C\right)w_t(p)\,dp$$

In (3), Δt is the time duration of each time interval (i.e., a market time unit), and $S_t(p)$ is the probabilistic profit for that time interval depending upon day-ahead and regulation prices $\left\{\lambda_t^D,\lambda_t^{up},\lambda_t^{dw}\right\}$, wind power generation p_t, day-ahead bidding B_t^D and reserves BS_t^C, BS_t^D. As the WF-ESS union is assumed to be a price taker in the electricity market, the day-ahead energy prices and up/down regulation prices are independent of its bidding and output. Consequently, the stochastic prices can be replaced by their expected value, and the expected profit at each interval can be expressed in the form of (3).

The expected profit at time interval t consists of three parts. The first part is the day-ahead bidding profit $\overline{\lambda}_t^D B_t^D$. The second part is the cost of purchasing up-regulation, which is negative in value, and the third part is the profit of selling down-regulation. To ensure the validity of the integral lower and upper limits, the bidding constraint $h\left(\boldsymbol{B^D},\boldsymbol{BS^C},\boldsymbol{BS^D}\right)\le 0$ reads:

$$0\le BS_t^C\le u_t^C\left(\overline{wf_t}-B_t^D\right)\quad \forall t\in\{1,2...T\} \qquad (4)$$
$$0\le BS_t^D\le u_t^D\left(B_t^D-\underline{wf_t}\right)\quad \forall t\in\{1,2...T\} \qquad (5)$$

There are also several operational constraints for the ESS, $g\left(\boldsymbol{BS^C},\boldsymbol{BS^D}\right)\le 0$, i.e.,

$$0\le BS_t^C\le u_t^C\overline{BS^C}\quad \forall t\in\{1,2...T\} \qquad (6)$$
$$0\le BS_t^D\le u_t^D\overline{BS^D}\quad \forall t\in\{1,2...T\} \qquad (7)$$
$$u_t^C+u_t^D\le 1\quad u_t^C,u_t^D\in\{0,1\}\quad \forall t\in\{1,2...T\} \qquad (8)$$
$$E_t=E_0+\sum_{j=1}^{t-1}BS_j^C\cdot\eta_C\cdot\Delta t-\sum_{j=1}^{t-1}BS_j^D/\eta_D\cdot\Delta t\quad \forall t\in\{1,2...T\} \qquad (9)$$
$$E_{\min}\le E_t\le E_{\max}\quad \forall t\in\{1,2...T\} \qquad (10)$$
$$E_T=E_0 \qquad (11)$$

where (6) and (7) constrain the charging and discharging power at time interval t within the charging and discharging capacity. Simultaneous charging and discharging is prevented by (8). The energy transition of the ESS is expressed in (9), and the residual energy should be within an allowable range $\left[E_{\min},E_{\max}\right]$ at any time interval with (10). As the model here is for daily operation, the residual energy deviation of ESS between the beginning and end of a day has great impact on daily profit. To evaluate the effect of the flexible charging and discharging capability of ESS on WF profit, the residual energy in ESS is constrained to be the same at the beginning and end of the day [8], as shown in (11). This strict constraint could be revisited in the future to provide more flexibility to the charging and discharging profiles for the ESS. Moreover, the ESS degradation effect is not included because we only consider daily operation. For long-term investment, the degradation can be complemented in the objective function as a cost, which relates to operation power and state of charge. It should also be noted that we propose the coordination strategies from the perspective of the wind-storage system, which is a participant in electricity markets, rather than from the perspective of a system operator. For example, participants in European zonal electricity markets usually do not pay special attention to network congestion. In case network constraints should be considered, the proposed model can be extended. In some situations, the wind farm and storage are co-located and connected to the same network bus. Then, constraints limiting joint output below the integration capacity C_{WF-ESS} can be added as,

$$B_t^D\le C_{WF-ESS},\ \overline{wf_t}-BS_t^C\le C_{WF-ESS}$$

Otherwise, the wind farm and storage are connected to different network buses, where similar constraints for output of wind farm C_{WF} and storage C_{ESS} can be added separately as follows,

$$B_t^D\le C_{WF},\ BS_t^C\le C_{ESS},\ BS_t^D\le C_{ESS}$$

IV. Solution Method

Instead of using scenarios, we adopt a probabilistic distribution to model wind power uncertainty in a more accurate way. As integration is included in the objective function (3) and binary variables are included in (4) through (8), the formulation is a mixed integer non-linear model and cannot be solved directly. In this paper, the gradient descent algorithm is modified according to the characteristics of the formulation. It should be noted that as the problem may be nonconvex, in that case, the proposed algorithm will only obtain the nearest local optimal solution rather than the global solution. The situation is the same for other popular algorithms such as the interior-point method. However, the computational effort required for the proposed algorithm is considerably less than metaheuristic algorithms, e.g., genetic algorithms, which can only theoretically obtain global optimal solutions. On the contrary, the stable and computation-friendly characteristics of the modified gradient descent algorithm make it easy to use in application and suitable for integration into rolling optimization. More importantly, by choosing proper initial points, the algorithm can obtain a satisfactory solution in an effective way. Another way is to try different initial solutions. As the proposed algorithm is computationally friendly, a number of initial solutions can be tried to obtain a better solution.

A. *Framework of the Algorithm*

The proposed algorithm is illustrated as follows.

Algorithm: Modified Gradient descent Algorithm

Begin:

$$\left\{\boldsymbol{B^{D0}},\boldsymbol{BS^{D0}},\boldsymbol{BS^{C0}}\right\}=\left\{\boldsymbol{W}^{-1}\left(\frac{\overline{\lambda}^D-\overline{\lambda}^{dw}}{\overline{\lambda}^{up}-\overline{\lambda}^{dw}}\right),0,0\right\}$$

$$S^0=f\left(\boldsymbol{B^{D0}},\boldsymbol{BS^{D0}},\boldsymbol{BS^{C0}}\right)$$

for k=1 : K

Execute ***ESS module*** $\Rightarrow\left\{\left[\boldsymbol{\Delta BS^{Dk}},\boldsymbol{\Delta BS^{Ck}}\right]\right\}$

Execute ***Bidding module*** $\Rightarrow\left\{\boldsymbol{\Delta B^{Dk}}\right\}$

$\boldsymbol{B^{Dk}}=\boldsymbol{B^{D(k-1)}}+\boldsymbol{\Delta B^{Dk}}$

$\boldsymbol{BS^{Dk} = BS^{D(k-1)} + \Delta BS^{Dk}}$

$\boldsymbol{BS^{Ck} = BS^{C(k-1)} + \Delta BS^{Ck}}$

$S^k = f\left(\boldsymbol{B^{Dk}, BS^{Dk}, BS^{Ck}}\right)$

if $S^k - S^{(k-1)} < 0$

Execute ***back-tracking procedure***:

$\gamma = 1$, $S^k(1) = S^k$

while $S^k(\gamma) \le S^{k-1}$

$\gamma = \beta\gamma$

$\boldsymbol{BS^{Dk}}(\gamma) = \boldsymbol{BS^{D(k-1)}} + \left(1-(1-\gamma)\boldsymbol{u^{Dk}}\right)\boldsymbol{\Delta BS^{Dk}}$

$\boldsymbol{BS^{Ck}}(\gamma) = \boldsymbol{BS^{C(k-1)}} + \left(1-(1-\gamma)\boldsymbol{u^{Ck}}\right)\boldsymbol{\Delta BS^{Ck}}$

$\boldsymbol{B^{Dk}}(\gamma) = \boldsymbol{B^{D(k-1)}} + \gamma\boldsymbol{\Delta B^{Dk}}$

$S^k(\gamma) = f\left(\boldsymbol{B^{Dk}}(\gamma), \boldsymbol{BS^{Dk}}(\gamma), \boldsymbol{BS^{Ck}}(\gamma)\right)$

end

$\boldsymbol{BS^{Dk} = BS^{Dk}}(\gamma)$, $\boldsymbol{BS^{Ck} = BS^{Ck}}(\gamma)$

$\boldsymbol{B^{Dk} = B^{Dk}}(\gamma)$, $S^k = S^k(\gamma)$

else if $0 \le S^k - S^{(k-1)} \le \varepsilon$

stop

else

continue the loop

end

end

$\boldsymbol{BS^{D} = BS^{Dk}}$, $\boldsymbol{BS^{C} = BS^{Ck}}$, $\boldsymbol{B^{D} = B^{Dk}}$

end

In the algorithm, the initial bidding is the optimal quantile from wind power predictive densities, as performed in [3]. $\boldsymbol{W^{-1}}(\cdot)$ is the vector of $W_t^{-1}(\cdot)$. The parameter γ is the step size, whose initial value is one. The back-tracking factor β shortens the step size. The key point is that the modified back-tracking will not change the value of u_t^C and u_t^D. Take u_t^C for example. If $u_t^C(1) = 0$, then $BS_t^{Ck}(\gamma) = BS_t^{Ck}(1) = 0$, and $u_t^C(\gamma) = 0$. Otherwise, $BS_t^{Ck}(\gamma) = BS_t^{C(k-1)} + \gamma\Delta BS_t^{Ck} > 0$ and $u_t^C(\gamma) > 0$. In the following subsections B to D, the ESS and bidding modules are introduced.

B. Linear Approximation of the Objective Function

In (3), when the expected prices and wind power distributions are available through predictions, then $E\left[S_t(p) \mid \lambda_t^D, \lambda_t^{up}, \lambda_t^{dw}, \theta\right]$ is a function of B_t^D, BS_t^D, BS_t^C, denoted by $S\left(B_t^D, BS_t^D, BS_t^C\right)$. At any time interval *t*, the expected profit $S\left(B_t^D, BS_t^D, BS_t^C\right)$ can be linearly approximated as:

$$S\left(B_t^D, BS_t^D, BS_t^C\right) \approx S\left(B_t^{D0}, BS_t^{D0}, BS_t^{C0}\right) + \left[\frac{\partial S}{\partial B_t^{D0}}, \frac{\partial S}{\partial BS_t^{D0}}, \frac{\partial S}{\partial BS_t^{C0}}\right] \cdot \left[\Delta B_t^D, \Delta BS_t^D, \Delta BS_t^C\right]^T \quad (12)$$

and

$$\frac{\partial S_t}{\partial B_t^D} = \overline{\lambda}_t^D - \overline{\lambda}_t^{up} W_t\left(B_t^D - BS_t^D\right) - \overline{\lambda}_t^{dw}\left[1 - W_t\left(B_t^D + BS_t^C\right)\right]$$

$$\frac{\partial S_t}{\partial BS_t^D} = \overline{\lambda}_t^{up} W_t\left(B_t^D - BS_t^D\right),$$

$$\frac{\partial S_t}{\partial BS_t^C} = -\overline{\lambda}_t^{dw}\left[1 - W_t\left(B_t^D + BS_t^C\right)\right]$$

The first part of (12) is fixed, so the optimal solution of (12) can be obtained by solving the second part. Moreover, equations (4) and (5) are quadratic but can be converted to linear equations via an iterative procedure on the decision variables involved. More specifically, B_t^D is a decision variable in the bidding module, where the value of u_t^C, u_t^D is derived from application of the ESS module at previous iterations. Similarly, u_t^C, u_t^D are decision variables in the ESS module, while B_t^D is obtained from the previous iteration of the ESS module.

C. ESS Module

In this module, the decision variables all regard charging and discharging of the ESS. The superscript *k* stands for the iteration number *k*, where all of the parameters with superscript (*k*-1) are constants. The original formulations (2) through (11) can be re-interpreted as follows in this module,

$$\max \quad \sum_{t=1}^{T}\left(\frac{\partial S_t}{\partial BS_t^{D(k-1)}}\Delta BS_t^{Dk} + \frac{\partial S_t}{\partial BS_t^{C(k-1)}}\Delta BS_t^{Ck}\right) \quad (13)$$

$$\text{s.t.} \quad 0 \le BS_t^{C(k-1)} + \Delta BS_t^{Ck} \le u_t^{Ck}\overline{BS^C} \quad (14)$$

$$0 \le BS_t^{D(k-1)} + \Delta BS_t^{Dk} \le u_t^{Dk}\overline{BS^D} \quad (15)$$

$$0 \le BS_t^{C(k-1)} + \Delta BS_t^{Ck} \le u_t^{Ck}\left(\overline{wf_t} - B_t^{D(k-1)}\right) \quad (16)$$

$$0 \le BS_t^{D(k-1)} + \Delta BS_t^{Dk} \le u_t^{Dk}\left(B_t^{D(k-1)} - \underline{wf_t}\right) \quad (17)$$

$$u_t^{Ck} + u_t^{Dk} \le 1 \quad (18)$$

$$E_t^k = E_t^{k-1} + \sum_{j=1}^{t-1}\Delta BS_t^{Ck}\cdot\eta_C\cdot\Delta t - \sum_{j=1}^{t-1}\Delta BS_t^{Dk}/\eta_D\cdot\Delta t \quad (19)$$

$$E_{\min} \le E_t^k \le E_{\max} \quad (20)$$

$$E_T^k = E_0 \quad (21)$$

where only the ESS-related variables ΔBS_t^{Dk}, ΔBS_t^{Ck} are included in the objective function. Moreover, optimized bidding $\left\{B_t^{D(k-1)}\right\}$ of iteration (*k*-1) is used in (16) and (17). It can help avoid quadratic formations because the parameters of iteration (*k*-1) are constants in iteration *k*.

D. Bidding Module

In this module, the decision variables are bidding-related variables, and the objective function only contains the day-ahead bidding profit. This translates into the following optimization problem,

$$\max \quad \sum_{t=1}^{T}\frac{\partial S_t}{\partial B_t^{D(k-1)}}\Delta B_t^{Dk} \quad (22)$$

$$\text{s.t.} \quad B_t^{D(k-1)} + \Delta B_t^{Dk} \le \overline{wf_t} - BS_t^{Ck-1} - \Delta BS_t^{Ck} \quad (23)$$

$$BS_t^{D(k-1)} + \Delta BS_t^{Dk} + \underline{wf_t} \le B_t^{D(k-1)} + \Delta B_t^{Dk}. \quad (24)$$

Here, the latest information on charging and discharging, namely, the optimized charging and discharging reserve capacity from iteration *k* in the ESS module, is considered in the bidding block to accelerate the computation. The accelerating effect will be illustrated in Section V.B.

V. CASE STUDIES

In this section, two case studies, which will be introduced in subsection V.A, are performed. The first study is a three-

interval case, which is used to validate the proposed gradient descent algorithm in computation efficiency and optimality. Detailed results are gathered in V.B. Furthermore, the second case is based on realistic data from the Nord pool market and a wind farm in Denmark. The influence of wind power correlation on the profit brought by the proposed strategy is analyzed in V.C, and the profit of the proposed strategy is compared with some other commonly adapted strategies in V.D.

A. Case Design

1) Case 1:

In the first case, only three time intervals are considered for the sake of simplicity and transparency. The data are given in Table I and Table II.

Table I Parameters of the WF-ESS union

η_C	η_D	$E_{\min}\ [MWh]$	$E_{\max}\ [MWh]$
0.9	0.9	1	10
$E_0\ [MWh]$	$\overline{BS^C}\ [MW]$	$\overline{BS^D}\ [MW]$	β
5	10	10	0.1

Table II Parameters of the market prices

Time interval	$\overline{\lambda}^{D}\ [DKK/kWh]$	$\overline{\lambda}^{dw}\ [DKK/kWh]$
1	0.4	0.2
2	0.8	0.7
3	0.6	0.5
$\overline{\lambda}^{up}\ [DKK/kWh]$	$\overline{Wf}\ [MW]$	$\underline{Wf}\ [MW]$
0.5	90	0
1.0	60	0
0.7	75	0

It is assumed that potential wind power generation obeys a uniform distribution. Because there is no limit on the distribution in (12), other distributions can also be adapted to the proposed method. The assumption of uniformity is not very grounded, but it is the simplest, especially when integrated into objective functions. The main purpose of employing a uniform distribution here is to compare the optimality of the proposed algorithm with commercial software such as CPLEX. Substituting $p \to U\left(\underline{wf_t}, \overline{wf_t}\right)$ into (3), the objective function is

$$S_t = \overline{\lambda}_t^D B_t^D - \frac{\overline{\lambda}_t^{up}}{2\overline{wf_t}}\left(B_t^D - BS_t^D\right)^2 + \frac{\overline{\lambda}_t^{dw}}{2\overline{wf_t}}\left(\overline{wf_t} - B_t^D - BS_t^C\right)^2. \quad (25)$$

Together with constraints (4) through (11), a quadratic formulation is built and solved by CPLEX.

2) Case 2:

In this case, wind power probabilistic forecasts are based on the forecast data for wind farms in Denmark. Details of the scenario generation methods can be found in [22] and [23], and data from wind scenarios can be downloaded from the website [24]. The original data have per-unit values and can be transferred to actual values by multiplying the capacity of the wind farm, which is set as 100 MW in this case. The day-ahead prices and up/down regulation prices for the DK-West area in the Nord Pool market on January 1st, 2014 are used. The price data are available at [25], and the data for the ESS are the same as in Table I.

B. Validation of the Proposed Algorithm

The optimal solutions for Case 1 are listed in Table III. It can be seen from Table III that with the coordination of ESS and WF, the union tends to bid a higher amount in the day-ahead market. As the price in period 2 is higher, the ESS sets some discharging reserve in this period and charging reserve in periods 1 and 3. The increasing amount of bidding in period 2 is also considerably higher than that of periods 1 and 3.

Table III Comparison of the bidding results

Interval	1	2	3
Bidding without ESS [MW]	60.0	20.0	37.5
Bidding with ESS [MW]	63.7	47.0	48.5
Charging reserve of ESS [MW]	5.6	0	4.4
Discharging reserve of ESS [MW]	0	8.1	0

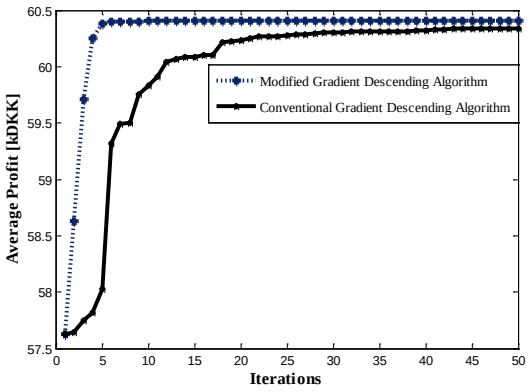

Fig. 3 Comparison on the converging process between conventional and modified gradient descent algorithms

As the latest information $\left\{\Delta BS_t^{Ck}, \Delta BS_t^{Dk}\right\}$ of charging and discharging reserve is utilized in the bidding module, the converging speed of the proposed algorithm is considerably faster than the conventional gradient descent algorithm, which only uses the information of $BS_t^{C(k-1)}$, $BS_t^{D(k-1)}$ in iteration k (replace ΔBS_t^{Ck}, ΔBS_t^{Dk} by $\Delta BS_t^{C(k-1)}$, $\Delta BS_t^{D(k-1)}$ in (23) and (24)). As shown in Fig. 3, it takes the modified gradient descent algorithm fewer than six iterations to reach convergence, and its value is 60.41 *k*DKK. Meanwhile, it takes the conventional algorithm over 40 iterations, with an objective value of 60.34 *k*DKK. The numeric results show that the proposed solving method is advantageous compared to the conventional gradient descent both in terms of converging speed and optimality.

The Hessian matrix of the objective function (25) is:

$$H_t = \begin{bmatrix} -\dfrac{\overline{\lambda}_t^{up} - \overline{\lambda}_t^{dw}}{\overline{wf}} & \dfrac{\overline{\lambda}_t^{up}}{\overline{wf}} & \dfrac{\overline{\lambda}_t^{dw}}{\overline{wf}} \\ \dfrac{-\overline{\lambda}_t^{up}}{\overline{wf}} & \dfrac{-\overline{\lambda}_t^{up}}{\overline{wf}} & 0 \\ \dfrac{\overline{\lambda}_t^{dw}}{\overline{wf}} & 0 & \dfrac{\overline{\lambda}_t^{dw}}{\overline{wf}} \end{bmatrix}. \quad (26)$$

As the third-order leading principal minor is positive, the Hessian matrix is not negative definite, so the problem is nonconvex. CPLEX only receives the upper bound, which is 60.60 *k*DKK. Meanwhile, the solution obtained with our proposed algorithm is 60.41 *k*DKK, which is quite close to that upper bound.

C. Influence of Wind Power Correlation

In the optimization model, wind power generation at different intervals is assumed to obey specific distributions independently of each other. However, the wind power output at interval *t* will partially depend on that at interval (*t*-1). To consider the influence of correlation on wind power generation, two types of scenarios are generated for comparison based on the data of the second case. For the first type, wind power at each interval is sampled independently and only obeys the predictive distributions for each time interval. The second type of scenario accounts for not only properties of predictive distributions at each time interval but also correlation between intervals. The method proposed in [26] and [27] can satisfy the requirement but can only simulate the scenarios with positive correlation. The first-order autoregressive process applied in [28] can set positive or negative values for the correlation of wind power forecast errors between intervals. In this paper, we combine the advantages of these two methods and generate scenarios satisfying the distribution and the correlation. The generation method is as follows:

i). One uses a Gaussian random number generator to have *K* realizations $\left\{\varepsilon_k^t\right\}$ for each of the *T* intervals, which are independent and identically distributed, $\varepsilon_k^t \sim N\left(\mu,\sigma^2\right)$

ii). Based on the uncorrelated realizations of step i), correlated realizations $\tilde{\varepsilon}_k^t$ can be generated through:

$$\begin{aligned}\tilde{\varepsilon}_k^1 &= \varepsilon_k^1 \\ \tilde{\varepsilon}_k^t &= \rho\tilde{\varepsilon}_k^{t-1} + \sqrt{1-\rho^2}\,\varepsilon_k^t\end{aligned} \tag{27}$$

where the autoregressive factor ρ can be set from [-1,1].

iii). For each interval *t*, apply the inverse probit function

$$\phi(\varepsilon) = \frac{1}{2}\left(1+erf\left(\frac{\varepsilon-\mu}{\sqrt{2}\sigma}\right)\right) = \frac{1}{2}\left(1+\frac{2}{\sqrt{\pi}}\int_0^{(\varepsilon-\mu)/\sqrt{2}\sigma} e^{-t^2/2}dt\right)$$

to each of $\left\{\tilde{\varepsilon}_k^t\right\}$, and *K* realizations $\left\{Y_k^t\right\}$ can be obtained.

iv). Apply the inverse cumulative distribution function of the day-ahead probability forecast $W_t^{-1}(\cdot)$ to each component of $\left\{Y_k^t\right\}$, and simulated wind power $\left\{p_k^t\right\}$ can be obtained.

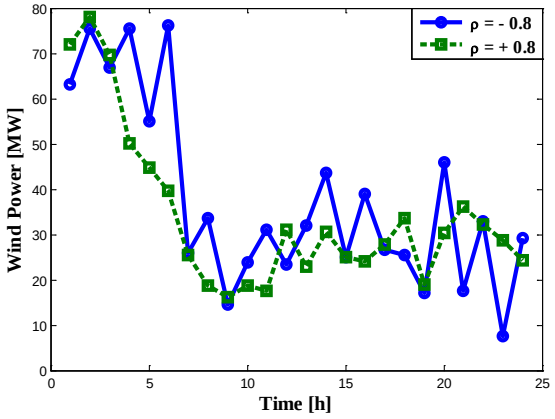

Fig. 4 Wind scenarios of different correlation factors

In the scenarios generation method, information on predictive distributions at each time interval $w_t(p)$ and the autoregressive factor ρ are necessary. Predictive distributions are fitted from the realistic data available, and the autoregressive factor ρ is uniformly sampled from [-1,1] to examine the influence of correlation on profit. Taking ρ equal to -0.8 and 0.8 for example, the corresponding wind power generation trajectories for the 24 market time units of the Nord Pool are illustrated in Fig. 4. It can be observed that the higher the correlation factor is, the smoother the resulting wind power trajectory is.

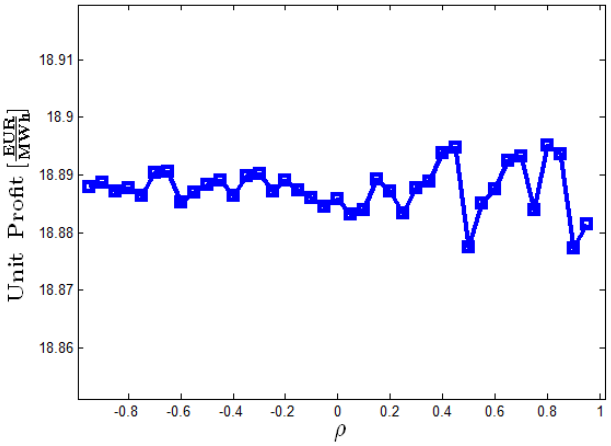

Fig. 5 The influence of wind power output correlation on unit profit as an average over all scenarios

As the wind power scenarios are generated randomly, the total wind energy may not be the same. For the sake of fairness, a new index, *unit profit*, is applied, which is defined as the overall profit from market participating per unit of wind energy generated. To study the influence of wind power correlation on profit brought by the proposed strategy, the autoregressive factor ρ increases from -1 to 1, with an increment of 0.05. For each value of ρ, 25,000 scenarios are generated to obtain the test results, consisting of the average outcome over this large number of scenarios. As shown in Fig. 5, the unit profit fluctuates slightly but remains steady regardless of ρ. This means that although the proposed strategy is based on the assumption of the non-correlation of wind power, it is still quite robust with respect to potential temporal dependence in wind power generation and forecast errors.

D. Comparison of Methods

Researchers in this field have already proposed several bidding and operation strategies on the coordination of WF and ESS. In this subsection, the proposed strategy is tested based on the realistic data for case 2 and is compared with the other three common strategies. These include:

- **Strategy 1**: *Expected Utility Maximization Strategy* [3]: the WF works alone, and the optimal bidding at interval *t* is $\left\{W_t^{-1}\left(\frac{\overline{\lambda}_t^D - \overline{\lambda}_t^{dw}}{\overline{\lambda}_t^{up} - \overline{\lambda}_t^{dw}}\right)\right\}$. The WF does not control its output and receives a penalty based on the imbalances.
- **Strategy 2**: *Filter Operation Strategy*: The WF-ESS union bids as Strategy 1 and uses the ESS to compensate

for the imbalance from WF as much as possible [13].

- **Strategy 3** *Reserve Operation Strategy*: The WF-ESS union bids as Strategy 1 but sets the operation reserve for the ESS [15].
- **Strategy 4**: *Proposed Bidding and Operation Strategy*: WF-ESS determines the day-ahead offering and operation reserve of ESS in an integrated way.

There are two types of tests used for that comparison, depending on whether the wind power correlation between intervals is considered in scenario generation. For both types of tests, one million scenarios are generated to obtain the test results.

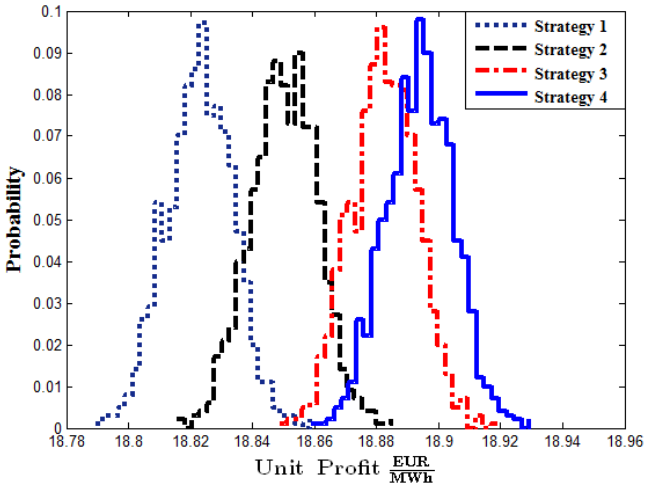

Fig. 6 The distributions of unit profit over uncorrelated scenarios for all strategies

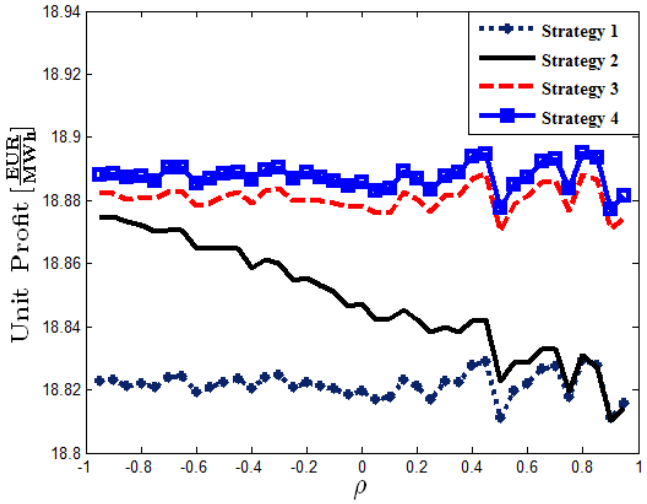

Fig. 7 The average unit profit over correlated scenarios for all strategies as a function of the autoregressive parameter

From Fig. 6, one can also observe that in the test that does not consider the correlation between the wind power output at neighboring intervals, strategies with ESS can obtain higher profit than Strategy 1, where the WF works alone. It is reasonable that for strategies with ESS, the ESS can help balance the deviation between wind power output and bidding, which reduces the deviation penalty. The situation is even better for Strategy 4 because ESS can also help make arbitrage to gain more profit. Consequently, Strategy 4 has a higher unit profit than other strategies.

Fig. 7 gathers the test results in cases where the wind power correlation is considered. The unit profit for the filter operating strategy (Strategy 2) decreases with an increase in correlation because when correlation becomes more positive, successive periods of similar positive or negative wind power deviations will happen more often. Then, the ESS will continuously charge or discharge, and the residual energy of the ESS will reach its upper or lower bounds more frequently. The ESS will fail in its imbalance compensation function eventually. It is natural that Strategy 1 is insensitive to the correlation because the ESS is not accounted for at the time of offering.

Combining the bidding strategy of Strategy 1 and the operation strategy of Strategy 4, Strategy 3 also has a slightly descending but steady unit profit with an increase in wind power correlation. This result comes from the hedge effect of the reserve-based real-time operation strategy because the charging and discharging power of ESS is determined by wind power deviation and is also constrained by predetermined reserve capacity. In all cases, Strategy 4 obtains the best results among all of the strategies. The comparison results inform us that (i) the correlation in wind power forecast errors has an influence on the performance of ESS (as Strategy 2) [28], and (ii) the proposed strategy appears to be robust, i.e., it is not negatively affected by these correlation effects.

VI. Conclusions

Integrated bidding and operation strategies for WF-ESS were proposed and evaluated. Meanwhile, a mixed integer nonlinear formulation was obtained and a modified gradient descent algorithm was designed for the practical numerical solution to these problems. Compared with the conventional gradient descent algorithm, the algorithm proposed in this paper converges faster and obtains better optimality. More importantly, the proposed bidding and operation strategies proved advantageous, in terms of unit profit and based on realistic data, compared to the three commonly used strategies from the literature. Case studies analyzing the potential impact of temporal correlation in wind power generation show that the proposed bidding and operating strategy is robust to these temporal dependence structure considerations.

Future work should naturally focus on improving the real-time operation strategy of ESS and WF (for instance, linear decision rules), while potential temporal dependence structures in wind power generation could be further considered in the bidding strategy. Moreover, the price-maker assumption of [29], [30] can be adopted, and ESS degradation should be considered. Furthermore, we plan to study the optimal sizing of ESS based on the proposed strategy to coordinate with wind farms.

VII. References

[1] C. J. Dent, J. W. Bialek, and B. F. Hobbs, "Opportunity cost bidding by wind generators in forward markets: analytical results," *IEEE Trans. Power Syst.*, vol. 26, no. 3, pp. 1600–1608, 2011.

[2] G. N. Bathurst, J. Weatherill, and G. Strbac, "Trading wind generation in short term energy markets," *IEEE Trans. Power Syst.*, vol. 17, no. 3, pp. 782–789, 2002.

[3] P. Pinson, C. Chevallier, and G. N. Kariniotakis, "Trading wind generation from short-term probabilistic forecasts of wind power," *IEEE Trans. Power Syst.*, vol. 22, no. 3, pp. 1148–1156, 2007.

[4] M. Zugno, T. Jõnsson, and P. Pinson, "Trading wind energy on the basis of probabilistic forecasts both of wind generation and of market quantities," *Wind Energy*, vol. 16, no. 6, pp. 909–926, 2013.

[5] M. D. Ilić, J. Y. Joo, L. Xie, M. Prica, and N. Rotering, "A decision-making framework and simulator for sustainable electric energy systems, " *IEEE Trans. Sustain. Energy*, vol. 2, no. 1, pp. 37–49, 2011.

[6] J. Hetzer, D. C. Yu, and K. Bhattarai, "An economic dispatch model incorporating wind power," *Energy Conversion, IEEE Trans.*, vol. 23, no. 2, pp. 603–611, 2008.

[7] H. Ding, Z. Hu, and Y. Song, "Stochastic optimization of the daily operation of wind farm and pumped-hydro-storage plant," *Renew. Energy*, vol. 48, pp. 571–578, 2012.

[8] H. Ding, Z. Hu, and Y. Song, "Rolling optimization of wind farm and energy storage system in electricity markets," *IEEE Trans. Power Syst.*, no. 99, pp. 1–9, 2014.

[9] E. D. Castronuovo and J. a P. Lopes, "On the optimization of the daily operation of a wind-hydro power plant," *IEEE Trans. Power Syst.*, vol. 19, no. 3, pp. 1599–1606, 2004.

[10] H. Bludszuweit and J. A. Domínguez-Navarro, "A probabilistic method for energy storage sizing based on wind power forecast uncertainty," *IEEE Trans. Power Syst.*, vol. 26, no. 3, pp. 1651–1658, 2011.

[11] M. Lu, C. Chang, W. Lee, and L. Wang, "Combining the wind power generation system with energy storage equipment," *IEEE Trans. Ind. Appl.*, vol. 45, no. 6, 2009.

[12] Y. Yuan, Q. Li, and W. Wang, "Optimal operation strategy of energy storage unit in wind power integration based on stochastic programming," *IET Renewable Power Generation*, vol. 5, no. 2. p. 194, 2011.

[13] E. D. Castronuovo, J. Usaola, R. Bessa, M. Matos, I. C. Costa, L. Bremermann, J. Lugaro, and G. Kariniotakis, "An integrated approach for optimal coordination of wind power and hydro pumping storage," *Wind Energy*, vol. 17, no. 6, pp. 829–852, 2013.

[14] P. Pinson, G. Papaefthymiou, B. Klöckl, and J. Verboomen, "Dynamic sizing of energy storage for hedging wind power forecast uncertainty," in *2009 IEEE Power and Energy Society General Meeting, PES '09*, 2009, pp. 1–8.

[15] E. Bitar, R. Rajagopal, P. Khargonekar, and K. Poolla, "The role of co-located storage for wind power producers in conventional electricity markets," *Proc. 2011 Am. Control Conf.*, pp. 3886–3891, 2011.

[16] G. N. Bathurst and G. Strbac, "Value of combining energy storage and wind in short-term energy and balancing markets," *Electr. Power Syst. Res.*, vol. 67, no. 1, pp. 1–8, 2003.

[17] H. Ding, Z. Hu, and Y. Song, "Optimal intra-day coordination of wind farm and pumped-hydro-storage plant," in *2014 IEEE PES General Meeting | Conference & Exposition*, 2014, pp. 1–5.

[18] A. Skajaa, K. Edlund, and J. M. Morales, "Intraday trading of wind energy," *IEEE Trans. Power Syst.*, pp. 1–9, 2015.

[19] J. García-González, R. M. R. de la Muela, L. M. Santos, and A. M. Gonzalez, "Stochastic joint optimization of wind generation and pumped-storage units in an electricity market," *IEEE Trans. Power Syst.*, vol. 23, no. 2, pp. 460–468, 2008.

[20] J. M. Morales, A. J. Conejo, H. Madsen, P. Pinson, and M. Zugno, *Integrating Renewables in Electricity Markets - Operational Problems*. Springer, 2014.

[21] M. Zugno, J. M. Morales, P. Pinson, and H. Madsen, "Pool strategy of a price-maker wind power producer," *IEEE Trans. Power Syst.*, vol. 28, no. 3, pp. 3440–3450, 2013.

[22] P. Pinson, "Wind energy: forecasting challenges for its operational management," *Stat. Sci.*, vol. 28, no. 4, pp. 564–585, Nov. 2013.

[23] W. A. Bukhsh, C. Zhang, and P. Pinson, "A multiperiod OPF model under renewable generation uncertainty and demand side flexibility," *unpublished*.

[24] W. A. Bukhsh, "Wind scenarios - data for stochastic multiperiod optimal power flow problem." [Online]. Available: https://sites.google.com/site/datasmopf/wind-scenarios. [Accessed: 07-Apr-2015].

[25] Energinet, "Download of market data." [Online]. Available: http://energinet.dk/EN/El/Engrosmarked/Udtraek-af-markedsdata/Sider/default.aspx. [Accessed: 07-Apr-2015].

[26] N. Troldborg and J. Sørensen, "A simple atmospheric boundary layer model applied to large eddy simulations of wind turbine wakes," *Wind Energy*, vol. 17, no. April 2013, pp. 657–669, 2014.

[27] Á. J. Duque, E. D. Castronuovo, I. Sánchez, and J. Usaola, "Optimal operation of a pumped-storage hydro plant that compensates the imbalances of a wind power producer," *Electr. Power Syst. Res.*, vol. 81, no. 9, pp. 1767–1777, 2011.

[28] P. Haessig, B. Multon, H. Ben Ahmed, S. Lascaud, and P. Bondon, "Energy storage sizing for wind power: Impact of the autocorrelation of day-ahead forecast errors," *Wind Energy*, 2013.

[29] L. Baringo and A. J. Conejo, "Strategic offering for a wind power producer," *IEEE Trans. Power Syst.*, vol. 28, no. 4, pp. 4645–4654, 2013.

[30] S. J. Kazempour and H. Zareipour, "Equilibria in an oligopolistic market with wind power production," *IEEE Trans. Power Syst.*, vol. 29, no. 2, pp. 686–697, 2014.